

Alina Carabello\*, Constanze Neupetsch, Dirk Zajonz, Michael Werner, Christian Rotsch, and Welf-Guntram Drossel

# Comparison of Resistive and Optical Strain Measurement for Early Fracture Detection

<https://doi.org/10.1515/cdbme-2020-3050>

**Abstract:** To increase learning success in surgical training, physical simulators are supplemented by measurement technology to generate and record objective feedback and error detection. An opportunity to detect fractures following hip stem implantation early can be measurement of occurring strains on bone surface. These strains can be determined while using strain gauges, digital image correlation (DIC) or photoelasticity. In this research strain gauges and DIC were compared regarding their suitability as strain measurement tools for use in physical simulators. Therefore a testing method was described to replicate the implantation of a hip stem. Testing devices modelled on a realistic prosthesis were pressed into prepared porcine femora in a two-step procedure with a material testing machine. The local strains occurring on bone surface were determined using an optical measurement system for DIC and strain gauges. The initial fractures in the tested femora are located medial-anterior in most cases (73,6%). With increasing indentation depth of the test device, the strains on bone surface increase. Comparing the local strains determined by DIC and strain gauges consistencies in curves are noticeable. Maximal determined strains before fracturing amount to 0,69% with strain gauges and 0,75% with DIC. In the range of the fracture gap, strain gradients are determined by using DIC. However the detected surfaces are of low quality caused by gaps and motion artefacts. The results show strains on bone surfaces for early fracture detection are measurable with strain gauges and DIC. DIC is assessed as less suitable compared to strain gauges. Furthermore strain gauges have greater level of integration and economic efficiency, so they are preferred the use in surgical training simulators.

**Keywords:** strain measurement, bone, strain gauges, digital image correlation, fracture

\*Corresponding author: Alina Carabello, Chemnitz University of Technology, Professorship for Adaptronics and Lightweight Design in Production, Chemnitz, Germany, e-mail: [alina.carabello@mb.tu-chemnitz.de](mailto:alina.carabello@mb.tu-chemnitz.de)

Constanze Neupetsch, Michael Werner, Christian Rotsch, Welf-Guntram Drossel, Fraunhofer Institute for Machine Tools and Forming Technology IWU, Chemnitz/Dresden, Germany  
Dirk Zajonz, Zeisigwaldkliniken BETHANIEN, Chemnitz, Germany

## 1 Introduction

The treatment of a hip joint with an endoprosthesis is a main area of surgical orthopaedics and requires extensive anatomical knowledge and experience to ensure the treatment of patients without complications. For these purposes physical simulators are used in surgical training. To increase learning success, integration of appropriate measurement technology can generate an objective feedback for the user and enable an early error detection. [9]

In literature no methods are described with regard to early error detection of intraoperative fractures following hip stem implantation. Thereby strains, that lead to fractures and occur when a prosthesis is impacted, can be measured with strain gauges and optical measurements. [1, 7]

Strain gauges are accurate measuring tools for determining local strains. Due to their size, strain gauges have a high degree of integration and are cost-effective compared to alternative methods e.g. optical measurements. For determining strain distributions on surfaces, several strain gauges are applied in an array. This results in increasing costs. [4, 7] Optical methods can contactless determine strain distributions with high local resolution. Disadvantageous are high costs for purchasing the measurement system and necessary visibility of the specimen. Photoelasticity also requires a complex coating of the specimen with photoelastic material, that can influence the mechanical behavior of the specimen. Also measuring accuracy depends on quality of the coating. [2] DIC, as an alternative optical method, requires texturing of the specimen with a speckle pattern instead of a photoelastic coating. Thereby the mechanical behavior of the test specimen is not affected. [4]

In this paper, DIC was examined for strain measurement on bone surface and was compared with strain gauges. The main goal was to identify a suitable strain measurement for use in a physical simulator. The determined strains are supposed to predict fractures. The requirements for the methodologies are low costs and accuracy. In order to reduce costs, the strain is to be determined locally at one measuring point. Artificial bone models with biomechanically correct behaviour are not yet available, but are already in development [6]. To be able to investigate a method for recording the strain, biological models are being used. The results can then be transferred to biomechanically correct bone models.

## 2 Materials and Methods

To assess the suitability of DIC and strain gauges, the strains occurring when an indentation test device is pressed into porcine femur on the basis of the implantation of a hip stem prosthesis, were determined. The preparation of specimen and experimental setup (s. fig. 1) imitated the process of hip stem implantation in laboratory environment under uniform boundary conditions. Therefore, two research objectives were pursued:

1. Localisation of occurring strains and fractures
2. Comparison of DIC and strain gauges

### 2.1 Specimen

Porcine femura show similarities to human femura with regard to their micro- and macrostructure and are suitable as animal models [8]. 19 porcine femura were tested: Specimen 1 to 14 were tested for localisation of occurring strains and fractures and five additional specimen (A to E) were tested for comparison of DIC and strain gauges. To connect the specimen to the test stand, they were embedded in a casting resin. The neck of the femur was cut with an oscillating bone saw and an adaptable additive manufactured template. The medullary cavity was opened with a rasp. A stochastic, isotropic and homogeneously speckle pattern for DIC was distributed with graphite dust over the measurement area.

### 2.2 Experimental Setup

A hip stem prosthesis from veterinary medicine was scaled and adapted to the dimensions of porcine femura for use as an indentation test device. Two models in different size were produced for testing and for generating fractures. To connect bone specimen with the material testing machine a positioning table with two degrees of freedom was used. It allowed the porcine femur to be aligned with the indentation test device.

The insertion of the indentation test device into the bone specimen was realized in a path-controlled manner with a material testing machine (DYNA-MESS Prüfsysteme GmbH, Aachen/Stolberg). For imitating the dynamic load, a crosshead speed of  $20 \text{ mm s}^{-1}$  was chosen. First, the indentation test device was pressed up to 75% into medullary cavity. If no fracture has occurred, it was pressed by a further 25%. So the indentation test device was completely pressed into the specimen.

To determine the localisation with increased incidence for fractures and occurring strains, 14 specimens were tested while using the optical measurement systems ARAMIS (GOM GmbH, Braunschweig, 12MP, measuring volume  $100 \times 80 \times 50 \text{ mm}$ ) and ATOS Core 300 (GOM GmbH, Braun-

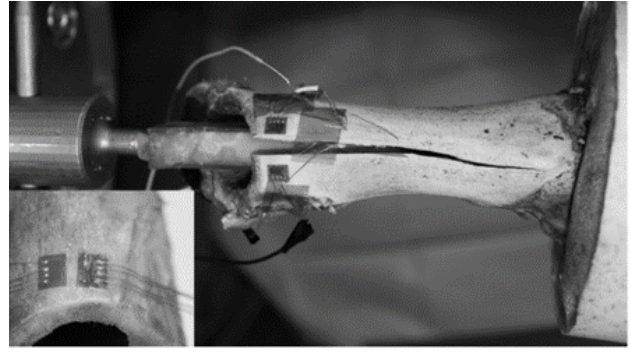


**Fig. 1:** Prepared porcine femora with fractures medio-anterior determined using DIC and strain gauges.

schweig, 5MP, measuring volume  $300 \times 230 \times 230 \text{ mm}$ ). They were positioned opposite each other and recorded the medial and lateral bone surfaces. Measurements were made with a maximum frame rate of 5 Hz. This was limited by the exposure time. Due to the camera setup, an exposure time of 65 ms was necessary. In addition five specimen were tested while only using the ARAMIS system, for the comparison of the methodologies of DIC and strain gauges. This allowed reducing exposure time and increasing frame rate up to 44 Hz.

The analysis of the image data was done with software „ARAMIS Professional 2017“. The image data were sampled with facet size of 13 pixels to identify the bone surface and generate a digital model. For quantification of occurring strains, the mean values of the axial and radial strains in the region of the fracture gap were calculated. For comparison of the results with the locally determined strains of the strain gauges, a curve was fitted to the digital bone surface in the area of the strain gauges. The elongation of this curve could be compared with the measurements of the strain gauges.

In addition to the speckle pattern, two biaxial strain gauges (Omega<sup>®</sup>, North Ireland,  $R_0 = 350 \Omega$ ,  $k = 2, 14$ ) each were applied to five femora at position 6 after classification according to Gruen [3]. They were connected to full bridges. Furthermore, a GSV-1M measurement amplifier and the NI-6009 USB box were used. The data acquisition rate was 100 Hz.

## 3 Results

Table 1 shows localisation of occurring fractures and quantification of largest axial and radial strains of each specimen before fractures occurred. 73,6% of specimens (14 out of 19) were fractured medio-laterally. The limitation of the indentation test device to two different sizes has thus proved to be insufficient, as 4 bones are not fractured. The applied speckle patterns allowed the bone surface to be identified (s. fig 2)

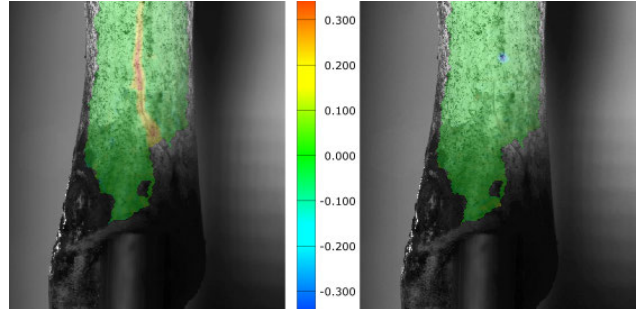
**Tab. 1:** Fracture localisation and optical quantification of the largest occurring strains for each specimen.

Femur	Fracture	Axial Strain [%]	Radial Strain [%]
1	medio-lateral	0,18	0,59
2	lateral	0,01	0,21
3	medio-lateral	0,16	0,79
4	medio-lateral	0,09	0,62
5	medio-lateral	0,05	0,59
6	medio-lateral	0,39	0,98
7	medio-lateral	0,11	0,72
8	none	0,05	0,16
9	none	0,01	0,18
10	medio-lateral	0,08	0,81
11	none	0,10	0,67
12	medio-lateral	0,07	0,79
13	medio-lateral	0,04	0,57
14	medio-lateral	n.a.	n.a.
A	medio-lateral	0,09	0,71
B	medio-lateral	0,13	0,67
C	medio-lateral	0,12	0,65
D	none	0,09	0,63
E	medio-lateral	0,10	0,75

except for specimen 14. Because of movement artefacts no surface could be detected. On the lateral side of the bones, neither axial nor radial strains can be determined, too. Maximum radial strains of  $0,62\% \pm 0,23\%$  are determined before the fracture gaps occurred, whereas the axial strains are up to  $0,1\% \pm 0,08\%$ . Due to the intervariability of the bone specimens, the values of local maxima differ between the bone specimen. This corresponds to the information given in the literature. Jasty et. al [5] have measured radial strains of up to 0.6% with strain gauges on human preparations, which leads to fractures and were larger than axially occurring strains.

Despite the use of two optical measuring systems, the dorsal and ventral sides of the bone are not detected. In addition, there is partial and complete loss of the speckle pattern in the area of the fracture. The image data show movement artefacts and blurring of the pattern. Furthermore, the exposure conditions have a negative effect on the calculation of the surfaces.

Figure 3 shows the curves of the strains over time. The strain values are plotted in separate diagrams for each specimen for comparing local strains determined with strain gauges and DIC to assess both methodologies. The DIC show an improved image quality in comparison with data generated with frame rate of 5 Hz. Despite the increased frame rate, motion artefacts have led to partial or complete loss of surface information which resulted in interruptions of the graphs. In each diagram an elongation plateau is shown in the first 1.8 s. During this time, the test device penetrates the bone specimen without acting on it. Then the strain increases over the time

**Fig. 2:** Radial (left) and axial (right) strains determined with DIC on medio-lateral porcine bone surface.

with increasing penetration depth. Bone specimen A to C are fractured during the first indentation step, while specimen E fractured during the second step and specimen D remained without fracture after two indentation steps. Thereby, the measurements were not stopped between the first and the second indentation stage, to record possible strain reductions over the time with constant load. In the graphs a decrease of strains determined with strain gauges can be seen. The optically determined strains remains constant. Despite the graphs of bone specimen B and D all graphs show local maximums when fracture occurred.

After fracturing strain values decrease. The optical measurement shows an irregular course, which is due to partial and complete losses of the speckle pattern as a result of the fracture gap. With resistive strain measurement, a plateau is reached after a view seconds. The decreasing strains can be explained by the reduction of the acting stresses after the fracture occurred. Deviations can be also seen in determined strain values between DIC and strain gauges. For instance the determined maximum strains of specimen A are 0,71% for optical and 0,69% for strain gauge measurement. In bone specimen B, an increase in the resistively determined strain up to 0,36% can be seen. The fracture develops after 2.2 s and was located below a strain gauge. The strain gauge was detached from the bone surface and could no longer provide valid measurement results, which is why the measurement is stopped after this time. In addition, there is a considerable loss of the speckle pattern due to a movement artefact.

Due to the low frame rate of 44 Hz in comparison to the penetration speed, strains can lead to losses of surface information. In addition, motion artefacts lead to an erroneous identification of the facets that are used for the calculation of the sample surface. This leads to errors in the calculation of the strains. This explains strain peaks at the edge of the surface information and the irregular course of the graphs of the locally determined strains.

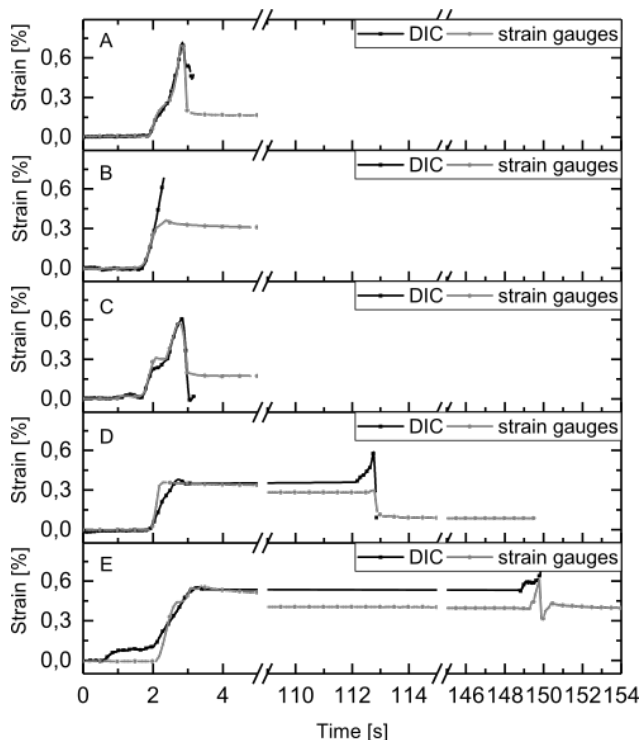


Fig. 3: Local strains determined with DIC and strain gauges.

## 4 Conclusion and Outlook

The results show that local strains and strain peaks resulting from the insertion of an indentation test device on bone surfaces can be determined with strain gauges and DIC. Deviations between strains determined with DIC and strain gauges are possible due to the non-linearity of strain gauges on high strains. Another aspect is the partial loss of surface information for DIC at the edge of the detected bone surface and in the fracture gap area. This can be caused by motion artefacts and strains between two images which could be too large to identify common facets and lead to losses of surface information or breaking up the speckle pattern through the fracture gap.

Both methods allow only localized measurement of the strains. Since the fractures occurred at the same location, the methodologies shown are suitable for this application according to hip stem. If the fracture behaviour is unknown, renewed preliminary examinations are necessary to define measuring points. Nevertheless the experiments show that strain gauges are a more stable measurement tool for determining local strains on bone surface before fracture occurs. Furthermore they have a greater level of economic efficiency and integration caused by the measurement principle without the need of an optical measurement system and their size. So strain gauges are assessed more suitable for early fracture detection compared to DIC.

Furthermore, it will be investigated whether the strains during implantation of a hip stem prosthesis can be used to identify critical strains for early fracture detection. Regarding to this, the suitability of strain gauges concerning their measuring frequency and local resolution is to investigate, too. Furthermore, the results shall be transferred to a realistic bone model [6]. This requires investigations with the appropriate material of the bone model. In further researches this bone models shall be used as surgical simulators with objective feedback.

### Author Statement

Research funding: The authors have no conflict of interest in relation to the present study. The conducted research is not related to either human or animals use. The work presented here will be co-financed with tax funds on the basis of the budget approved by the members of Parliament of Saxony (SAB FKZ 100334004, term: 04/18- 12/20).

## References

- [1] Elias JJ, Nagao M, Chu YH, Carbone JJ, Lennox DW, Chao EYS. Medial Cortex Strain Distribution During Noncemented Total Hip Arthroplasty. *Clinical orthopaedics and related research* 2000;250-258
- [2] Ellenrieder M, Steinhauser E, Bader R, Mittelmeier W. Influence of cementless hip stems on femoral cortical strain pattern depending on their extent of porous coating. *Biomedizinische Technik. Biomedical engineering* 2012;57:121-129
- [3] Gruen TA, McNeice GM, Amstutz HC "Modes of failure" of cemented stem-type femoral components: a radiographic analysis of loosening. *Clinical Orthopaedics and Related Research* 1979;141:17-27
- [4] Hoult NA, Take A, Andy Take, W, Lee C, Dutton M. Experimental accuracy of two dimensional strain measurements using Digital Image Correlation. *Engineering Structures* 2013; 46:718-726
- [5] Jasty M, Henshaw RM, O'Connor DO, Harris WH. High Assembly Strains and Femoral Fractures Produced During Insertion of Uncemented Femoral Components: A Cadaver Study. *The Journal of Arthroplasty* 1993;479-478
- [6] Neupetsch C, Hensel E, Werner M, Meißner S, Troge J, Drossel WG, et al. Development and Validation of Bone Models using Structural Dynamic Measurement Methods. *Current Directions in Biomedical Engineering* 2019;5(1):343-346
- [7] Miles AW, Tanner KE. *Strain Measurement in Biomechanics*. 1st ed. Springer Netherlands 1992
- [8] Pearce AJ, Richards RG, Milz S, Schneider E, Pearce S. G. Animal models for implant biomaterial research in bone: A review. *European Cells and Materials* 2007; 13:1-10
- [9] Sadideen H, Plonczak A, Saadeddin M, Kneebone R. How Educational Theory Can Inform the Training and Practice of Plastic Surgeons. *Plastic and reconstructive surgery*. 2018;12:20-42